Activity of mo(w)s-2/sba-15 catalysts synthesized from simow heteropoly acids in 4,6-dimethyldibenzothiophene hydrodesulfurization

Aleksandr Kokliukhin, M. S. Nikul'Shina, A. A. Sheldaisov-Meshcheryakov, A. V. Mozhaev, Christine Lancelot, Pascal Blanchard, Carole Lamonier, P. A. Nikul'Shin

Activity of $Mo(W)S_2$/SBA-15 Catalysts Synthesized from SiMoW Heteropoly Acids in 4,6-Dimethyldibenzothiophene Hydrodesulfurization

A. S. Koklyukhin[a, b], M. S. Nikul'shina[a], A. A. Sheldaisov-Meshcheryakov[a, b], A. V. Mozhaev[a], C. Lancelot[b], P. Blanchard[b], C. Lamonier[b], and P. A. Nikul'shin[a, c, *]

[a] *Samara State Technical University, Samara, 443100 Russia*

[b] *Université Lille1, UCCS, Cité Scientifique, Lille, 590000 France*

[c] *All-Russia Research Institute of Oil Refining, Moscow, 111116 Russia*

**e-mail: p.a.nikulshin@gmail.com*

Received June 3, 2019; revised July 9, 2019; accepted September 8, 2019

Abstract—Mo(W)/SBA-15 catalysts are prepared using heteropoly acids $H_4SiMo_{12}O_{40}$, $H_4SiW_{12}O_{40}$, and $H_4SiMo_3W_9O_{40}$. The catalysts in the sulfide form are studied by low-temperature nitrogen adsorption, high-resolution transmission electron microscopy, and X-ray photoelectron spectroscopy. Catalytic properties are tested in the hydrodesulfurization of 4,6-dimethyldibenzothiophene. It is shown that the gas-phase sulfiding of Mo(W)/SBA-15 catalysts leads to increase in the average length of particles and the number of $Mo(W)S_2$ layers in active phase particles compared with liquid-phase sulfiding with the use of dimethyl sulfide. The replacement of a quarter of tungsten atoms with molybdenum ones makes it possible to considerably improve the catalytic activity of the mixed catalyst Mo + W/SBA-15 compared with the monometallic counterparts. This effect can be enhanced due to the use of mixed heteropoly acid $H_4SiMo_3W_9O_{40}$ as a precursor of the active phase of the MoW/SBA-15 catalyst, which is apparently associated with the formation of $MoWS_2$ active sites.

Keywords: hydrotreatment, heteropoly acid, $MoWS_2$ active phase, 4,6-dimethyldithiobenzothiophene

DOI: 10.1134/S0965544119120077

The consumption of ultrapure motor fuels continues to grow, while the quality of the processed raw materials worsens considerably. Secondary fractions (up to 30% or above) are more frequently involved in the process of diesel fraction hydrofining [1, 2]; as a result, the proportion of hard-to-remove heteroatomic (dibenzothiophene derivatives) and aromatic compounds increases. These changes in the feedstock chemical composition are responsible for more strict requirements on deep hydrotreating catalysts, and demands for catalysts will only increase because of the current and long-term environmental standards restricting the content of sulfur and polycyclic aromatic hydrocarbons in motor fuels and lubricant oils [3, 4].

In recent years, the attention of researchers has been focused on the design of mixed hydrotreating catalysts including just two structure-forming active phase metals—molybdenum and tungsten. This interest is associated with a high catalytic activity of mixed $MoWS_2$ systems [4–6]. Oxide precursors of the sulfide active phase play a crucial role in the process of catalyst synthesis. Current research in this field more frequently concerns using molybdenum and tungsten Keggin structure heteropoly acids [7, 8] and their derivatives, which in turn show high solubility and stability and are in wide use in the industry. As was shown in [9], the formation of bimetallic MoW oxide precursors ensures formation of mixed metal sulfides, whereas in the case of the mechanical mixture two different Mo and W compounds particles of individual monometallic sulfides prevail on the surface of the $MoWS_2/Al_2O_3$ catalyst [9].

Catalytic activity is considerably affected not only by oxide precursors but also by the support used. The support nature influences the dispersity of catalyst oxide and sulfide phases, the size distribution of active component particles, and the degree of their sulfiding [6, 10]. The absolute leader among hydrotreating catalyst supports is Al_2O_3; however, information about advantages of mesostructured silica having a higher specific surface area, equal sizes of channels, which are nanoreactors for targeted chemical reactions, inactivity toward formation of low-activity sulfide particles, and thermal stability, has appeared in recent decades. The most widespread representatives of these materials are SBA-15 [11], MCM-41 [12], and HMS [13]. It was reported that CoMoS and $Mo(W)S_2$ catalysts deposited on SBA-15 show a higher activity in the hydrogenation and hydrodesulfurization reactions because of a high dispersity and optimal morphology of active-phase particles [14–16]. Mendoza-Nieto et al. [17] demonstrated that the activity of trimetallic

catalysts NiMoW/SBA-15 in the hydrodesulfurization (HDS) of dibenzothiophene and 4,6-dimethyldithiobenzothiophene (4,6-DMDBT) was higher compared with their counterparts deposited on Al_2O_3.

As was shown in [15], the monometallic catalysts MoS_2/SBA-15 and WS_2/SBA-15 and the bimetallic mixed sample (Mo + W)S_2/SBA-15, which were sulfided by the liquid-phase method with the use of dimethyl disulfide, exhibit a higher activity in the hydrodesulfurization of dibenzophiophene and naphthalene compared with Al_2O_3-deposited counterparts and are characterized by a better dispersity of active-phase particles. The goal of this study was the synthesis of the $MoWS_2$/SBA-15 catalyst with the use of mixed bimetallic heteropoly acid $H_4SiMo_3W_9O_{40}$ containing both metals in its anion as an oxide precursor and the comparison of composition and characteristics of sulfide particles on the surface of SBA-15-deposited catalysts with those of monometallic samples based on $H_4SiMo_{12}O_{40}$ and $H_4SiW_{12}O_{40}$ and the bimetallic counterpart prepared from the mechanical mixture of the mentioned heteropoly acids. The catalytic properties of the Mo(W)S_2/SBA-15 catalysts sulfided by the gas-phase method were studied in the 4,6-DMDBT hydrodesulfurization. This sulfur-containing compound was chosen because it concentrates in the high-boiling part of middle-distillate oil fractions and its activity is much lower active than that of dibenzothiophene because of steric hindrances to σ-adsorption on edge active sites.

EXPERIMENTAL

SBA-15 was synthesized in accordance with previously described techniques [18]. Triblock copolymer Pluronic P123 (M = 5800, EO20PO70EO20, Aldrich) was used as a structure-forming agent, and tetraethyl orthosilicate was used as a source of silica. A weighed portion of Pluronic P123 (4 g) was dissolved in water (30 cm^3) containing 2 M HCl (120 cm^3) at a temperature of 35°C. The weighed portion of tetraethyl orthosilicate (8.5 g) was added dropwise under vigorous stirring to the obtained solution, and the resulting mixture was held for 20 h at 35°C. After holding, the still solution was transferred to a polypropylene bottle (1000 cm^3) and placed in a thermostat for 48 h at a temperature of 80°C. The product was cooled to room temperature, filtered, washed with deionized water, dried at 60, 80, and 100°C for 5, 2, and 5 h, respectively; and finally calcined at 240 and 540°C for 4 and 6 h, respectively.

Mo(W)/SBA-15 catalysts were synthesized by the single incipient wetness impregnation of the synthesized SBA-15 with the solution of corresponding heteropoly acid followed by drying at 100°C for 12 h without calcination. Precursors were Keggin structure monometallic $H_4SiMo_{12}O_{40}$ and $H_4SiW_{12}O_{40}$ heteropoly acids and mixed heteropoly acid $H_4SiMo_3W_9O_{40}$ [19, 20]. All samples had the same surface concentration of metals (Mo + W) equal to ~1.2 at/nm^2.

To study the physicochemical properties the synthesized oxide samples were activated (sulfided) in a flow of H_2S/H_2 (10 vol % H_2S) under heating at a rate of 5°C/min followed by holding at 400°C for 2 h.

The textural characteristics of the catalysts were measured by low-temperature nitrogen adsorption on a Quantachrome Autosorb-1 adsorption porosimeter. The specific surface area was calculated according to the Brunauer–Emmett–Teller (BET) model at P/P_0 = 0.05–0.3. The total pore volume and pore size distribution were calculated from the desorption curve in terms of the Barrett–Joyner–Halenda model.

The composition of active-phase particles of the synthesized Mo(W)/SBA-15 catalysts in the sulfide form was studied by X-ray photoelectron spectroscopy on a Kratos Axis Ultra DLD spectrometer using AlK_α radiation (hν = 1486.6 eV). The samples were applied on a double-sided nonconducting adhesive tape. The charging effect arising during the photoemission of electrons was minimized through irradiation of the sample surface by a beam of low-energy electrons. The binding energy (E_b) scale was preliminarily calibrated against positions of the peaks of core levels Au $4f_{7/2}$ (84.0 eV) and Cu $2p_{3/2}$ (932.67 eV). Calibration was made against the C1*s* line (284.8 eV) of carbon present on the catalyst surface. The energy step was 1 eV for the survey spectrum and 0.1 eV for individual lines C 1*s*, Si 2*p*, S 2*p*, Mo 3*d*, and W 4*f*. For all sulfide catalysts the relative concentrations of W^{6+} (Mo^{6+}) particles in the oxide environment, oxysulfides WS_xO_y (MoS_xO_y), and sulfides WS_2 (MoS_2) were determined.

The catalyst samples in the sulfide form were also analyzed by high-resolution transmission electron microscopy (HR TEM) on a Tecnai G2 20 instrument at an accelerating voltage of 200 kV. Parameters, such as the average length of particles ($\bar{L}$) and the number of Mo(W)S_2 layers per stack ($\bar{N}$), were determined by the statistical treatment of 400–600 particles situated in 10–15 different areas of the catalyst surface. The dispersity (D) of active-phase particles was calculated in terms of the Kasztelan hexagonal model [21]:

$$D = \frac{M_e + M_c}{M_T} = \frac{\sum_{i=1..t} 6n_i - 6}{\sum_{i=1..t} 3n_i^2 - 3n_i + 1}, \quad (1)$$

where M_e is the number of Mo(W) atoms on the edges of middle crystallite Mo(W)S_2, M_c is the number of Mo(W) atoms on the corners of middle Mo(W)S_2 crystallite, M_T is the total number of Mo(W) atoms in the middle particle of the active phase; n_i is the number of Mo atoms along one side of the Mo(W)S_2 crystallite defined by its length; and t is the total number of stacks in the crystallite according to HR TEM.

The catalytic properties of the catalyst samples were tested in the process of 4,6-DMDBT (0.6 wt %) hydrodesulfurization in toluene in a flow unit equipped with a microreactor. A steel reactor was charged with the

catalyst (0.4 g, fraction 0.25–0.50 mm) diluted with carborundum at a ratio of 1 : 4. Tests were run under the following conditions: temperature, 320°C; pressure, 3.0 MPa; feed space velocity, 5–10 h^{-1}; and H_2 : feedstock, 500 nL/L. Before testing, the catalysts were sulfided in a flow of H_2S/H_2 (10 vol % H_2S) under heating at a rate of 5°C/min followed by holding at 400°C for 2 h. Liquid samples were analyzed by gas-liquid chromatography on a Kristall-5000 chromatograph.

The rate constant of 4,6-DMDBT hydrodesulfurization was calculated with allowance for the pseudo-first order of this reaction according to the following equation:

$$k_{HDS} = -\frac{F_{4,6\text{-DMDBT}}}{m}\ln(1 - x_{4,6\text{-DMDBT}}/100), \qquad (2)$$

where k_{HDS} is the rate constant (mol g^{-1} h^{-1}) of 4,6-DMDBT hydrodesulfurization, $x_{4,6\text{-DMDBT}}$ is the conversion of 4,6-DMDBT (%), $F_{4,6\text{-DMDBT}}$ is the molar consumption of the reagent (mol h^{-1}), and m is the catalyst weight (g).

The hydrogenation of 4,6-DMDBT aromatic rings (Scheme 1) followed by the hydrogenolysis of C–S–C bonds and the formation of methylcyclohexyltoluene and 3,3'-dimethylbicyclohexyl occurs at a rate several times higher than the rate of direct hydrogenolysis of C–S–C bonds accompanied by the formation of 3,3'-dimethylbiphenyl. This result be attributed to steric hindrances caused by methyl substituents, which hinder the σ-adsorption of a sulfur molecule on the active site. The reaction products contain only trace 4,6-tetrahydro- and perhydrodibenzothiophenes. The selectivity of the hydrogenation route for direct desulfurization $S_{HYD/DDS}$ was calculated in accordance with the reaction scheme of 4,6-DMDBT transformation:

$$S_{HYD/DDS} = \frac{C_{MCHT} + C_{DMBCH}}{C_{DMBP}}. \qquad (3)$$

The turnover frequency (TOF_{HDS}, s^{-1}) for the 4,6-DMDBT hydrodesulfurization over the edge sites of $Mo(W)S_2$ particles was calculated as follows [22]:

$$TOF_{HDS} = \frac{F_{4,6\text{-DMDBT}}x_{4,6\text{-DMDBT}}}{m\left(\frac{C_{WS_2}}{Ar_W} + \frac{C_{MoS_2}}{Ar_{Mo}}\right)D \times 3600}, \qquad (4)$$

where $F_{4,6\text{-DMDBT}}$ is the consumption of 4,6-DMDBT (mol h^{-1}); $x_{4,6\text{-DMDBT}}$ is the conversion of 4,6-DMDBT (%); m is the catalyst weight (g); C_{WS_2} and C_{MoS_2} is the content (wt %) of W and Mo in WS_2 and MoS_2 particles, respectively; D is the dispersity of $Mo(W)S_2$ particles; and Ar_W and Ar_{Mo} are the atomic masses of tungsten (183.9 g/mol) and molybdenum (95.9 g/mol).

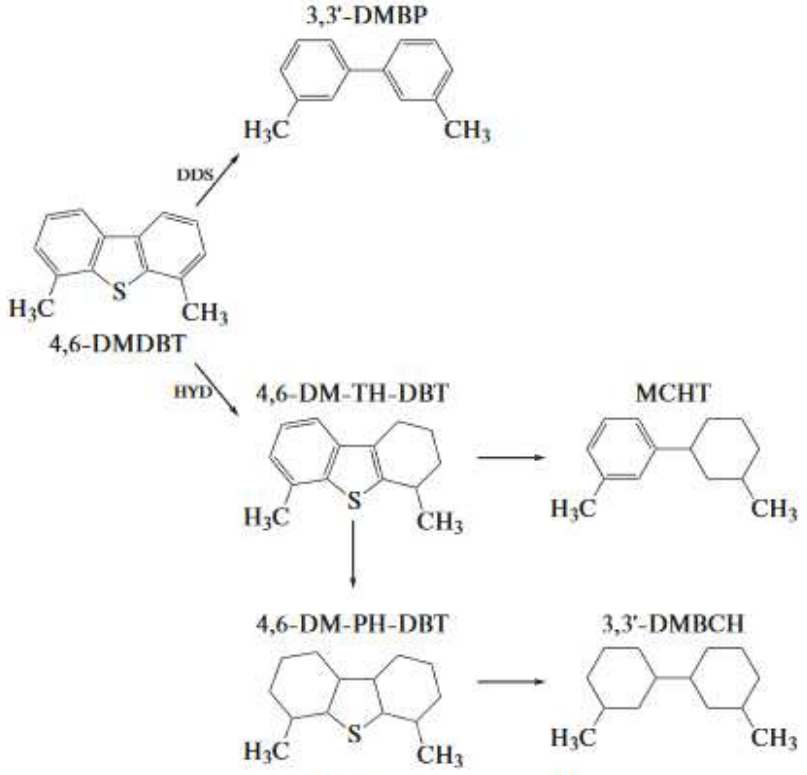

Scheme 1. Routes of 4,6-dimethyldibenzothiophene hydrodesulfurization, HYD is the preliminary hydrogenation path, and DDS is the path via the direct removal of sulfur atoms (3,3'-DMBP is 3,3'-dimethylbiphenyl, 4,6-DMDBT is 4,6-dimethydibenzothiophene, 4,6-DM-TH-DBT is 4,6-dimethyltetrahydrodibenzothiophene, MCHT is methylcyclohexyltoluene, 4,6-DM-PH-DBT is 4,6-dimethylperhydrodibenzothiophene, and 3,3'-DMBCH is 3,3'-dimethylbicyclohexyl).

RESULTS AND DISCUSSION

The composition and textural characteristics of the synthesized samples and the geometry characteristics of active-phase particles are shown in Table 1. The original SBA-15 possessed high specific surface area (850 m^2/g) and pore volume (1.18 cm^3/g). Naturally, after metal deposition the specific surface area decreased to 450–500 $м^2/g$ and the pore volume decreased to 0.55–0.80 cm^3/g.

The TEM images of the sulfide catalysts are shown in Fig. 1. Black threadlike bands correspond to the layers of $Mo(W)S_2$ crystallites with a characteristic interplanar distance of about 0.65 nm [23].

It should be noted that the Mo(W)/SBA-15 catalysts sulfided by the gas-phase method are characterized by a larger average number of $Mo(W)S_2$ layers in a crystallite and a larger average length of crystallites compared with the catalysts sulfided by the liquid-phase method. The dispersity of particles for the Mo(W)/SBA-15 samples sulfided by the gas-phase method was lower and amounted ~0.28 against ~0.32 for the samples sulfided by the liquid-phase method. These changes are apparently related to different sulfiding kinetics of oxide particles: in the case of the gas-phase method, as is known [24], the transformations of supported oxide precursors begin at room temperature to form oxysulfides and subnanosized MoS_3 particles, which further at higher temperatures (>300°C) convert to two-dimensional MoS_2 crystallites. As regards the liquid-phase activation process, the catalyst sulfiding starts at 170–220°C—the decomposition temperatures of the sulfiding agent—and the formation of active-component particles is coupled with the catalyst running-in by the feedstock and the stabilization of the formed nanosized particles by amorphous carbon. As a result, the number of $Mo(W)S_2$ layers in the stack in the case of the liquid-phase method is smaller compared with the gas-phase method.

The TEM images show small rounded dark spots which are particles of the unreacted precursor or oxysulfide phases [11]. Almost all active-phase particles are localized inside support channels, as is also seen from the images. The average length of $Mo(W)S_2$ particles is not above 5 nm, which is evidently related to the size of SBA-15 channels (5.6 nm) hampering the growth of sulfide particles in the process of catalyst sulfiding.

The composition of particles on the surface of the synthesized catalysts was investigated in detail by X-ray photoelectron spectroscopy (Table 2). The tested samples possess a high degree of metal sulfiding. A high degree of tungsten sulfiding should be mentioned (above 60 rel. %), which is, however, slightly lower than the degree of molybdenum sulfiding in Mo_{12}/SBA-15 (74 rel. %). Molybdenum in the MoW/SBA-15 samples fully passes to the sulfide phase during the process of catalyst sulfiding because of its small content in the samples and a high sulfiding rate.

The content of edge active sites on the catalyst surface was determined which for the synthesized samples varied within $0.32–0.60 \times 10^{20}$ at/g. The activation method (gas-phase or liquid-phase) insignificantly affected the degree of metal sulfiding. These results are consistent with the data obtained for the catalysts synthesized on alumina [9].

The data on the catalytic activity of the Mo(W)/SBA-15 catalysts in the 4,6-DMDBT hydrodesulfurization are summarized in Table 3. The reactant conversion varied from 11.7 to 43.5%. The lowest activity in all the studied reactions was exhibited by the sample prepared from SiW_{12}HPA. This can be explained by a low content of active sites and a lower degree of tungsten sulfiding because of a stronger W–O bond. The sample synthesized using the mechanical mixture of monometallic heteropoly acids ($Mo_3 + W_9$)/SBA-15 exhibited a higher catalytic activity compared with Mo_{12}/SBA-15 with the content of active sites being comparable (Table 2). These results can be probably explained by the enhanced hydrating function owing to the presence of tungsten in the sample. The Mo_3W_9/SBA-15 catalyst provided the maximal 4,6-DMDBT conversion (43.5%) among the tested samples; in this case, the content of edge active sites was the smallest.

To level off the amount of active-phase particles in the synthesized catalysts the turnover frequencies (TOF) normalized to the content of edge active sites in the $Mo(W)S_2$ crystallites was calculated (Fig. 2).

In the 4,6-DMDBT hydrodesulfurization the samples based on monometallic heteropoly acids and their mechanical mixtures demonstrated comparable turnover frequencies (about $8 \times 10^{-4}\ s^{-1}$). However, for the Mo_3W_9/SBA-15 sample prepared using of the mixed heteropoly acid $H_4SiMo_3W_9O_{40}$ the turnover frequency was more than two times higher than the respective value for the mixed counterpart. This finding provides evidence for formation of the mixed sulfide phase $MoWS_2$ which is more active than conventional catalytic systems. Actually, the application of high-angle annular dark-field scanning transmission electron microscopy (HAADF) and extended X-ray absorption fine structure spectroscopy (EXAFS) revealed that the use of the Keggin structure mixed $SiMo_3W_9$ heteropoly acid as an oxide precursor of the MoW/Al_2O_3 hydrotreating catalyst provides the spatial proximity of Mo and W atoms and thus facilitates formation of the mixed $MoWS_2$ phase with the even inclusion of Mo atoms in the structure of WS_2 crystallites [9, 25, 26].

Thus, we showed that for the Mo(W)/SBA-15 catalysts the use of gas-phase sulfiding makes it possible to increase the average length of sulfide particles and the average number of layers in the $Mo(W)S_2$ stack

Table 1. Composition, textural characteristics, and morphology of sulfide particles for the synthesized Mo(W)/SBA-15 catalysts

Catalyst	Content, wt %		Textural characteristics			Geometry characteristics		
	MoO_3	WO_3	surface area S_{BET}, m^2/g	pore volume V_p, cm^3/g	pore diameter $\varnothing$, nm	average particle length $\bar{L}$, nm	average number of $Mo(W)S_2$ layers in crystallite $\bar{N}$	dispersity of $Mo(W)S_2$ particles, D
SBA-15	–	–	850	1.18	5.6	–	–	–
Mo_{12}/SBA-15	18.0	–	492	0.68	5.6	4.1 (3.8)[a]	2.7 (2.1)[a]	0.29
W_{12}/SBA-15	–	26.2	453	0.55	5.6	4.4 (3.5)	2.6 (1.9)	0.27
Mo_3W_9/SBA-15	4.2	20.1	452	0.78	5.6	3.9 (3.6)	2.3 (2.1)	0.30
(Mo_3+W_9)/SBA-15	4.2	20.1	447	0.64	5.6	4.1 (3.8)	2.7 (2.0)	0.29

[a] The parenthesized values refer to the catalysts sulfided by the liquid-phase method [15].

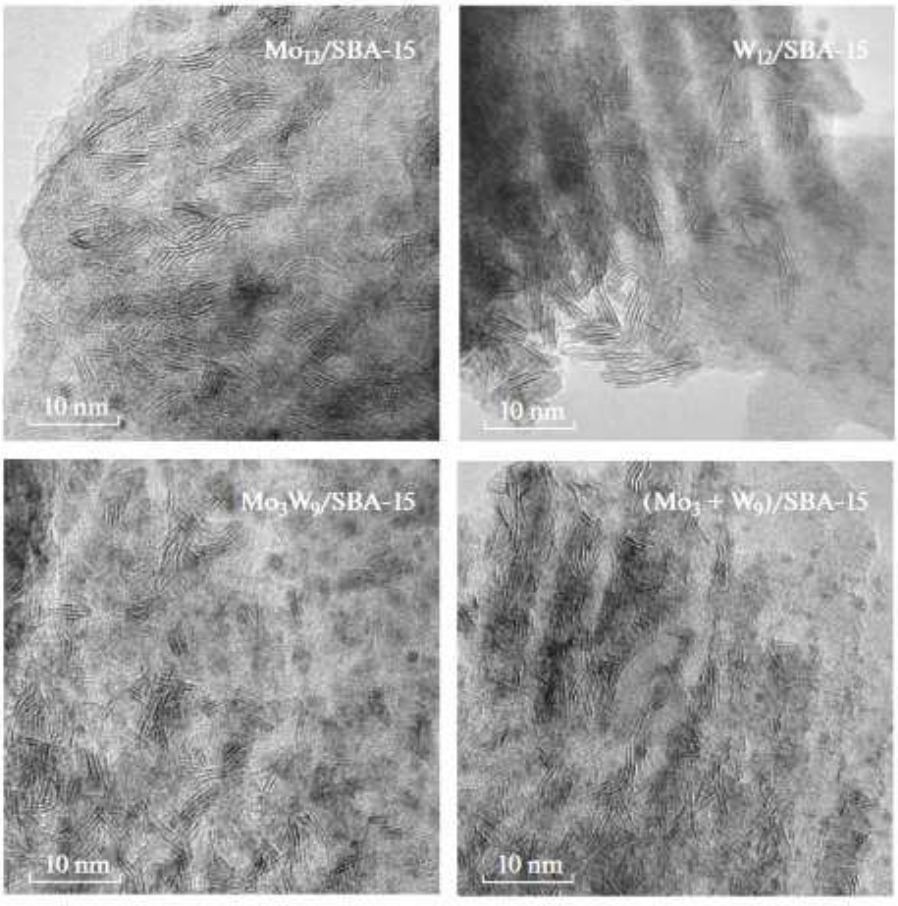

Fig. 1. TEM images of the sulfided Mo(W)/SBA-15 catalysts.

Table 2. Surface composition of active-phase particles of sulfided Mo(W)/SBA-15 catalysts according to transmission electron microscopy and X-ray photoelectron spectroscopy

Catalyst	Content of Mo, rel. %			Content of W, rel. %			Number of edge sites, 10^{20} at g^{-1}		
	MoS_2	MoS_xO_y	Mo^{6+}	WS_2	WS_xO_y	W^{6+}	Mo^{IV}_{edge}	W^{IV}_{edge}	$\Sigma Mo^{IV}_{edge} + W^{IV}_{edge}$
Mo_{12}/SBA-15	74 (73)[a]	13 (12)	14 (15)	–	–	–	0.56	0.00	0.56
W_{12}/SBA-15	–	–	–	61 (67)	12 (9)	25 (24)	–	0.32	0.32
Mo_3W_9/SBA-15	95 (100)	3 (0)	2 (0)	64 (65)	14 (8)	22 (27)	0.14	0.25	0.39
(Mo_3+W_9)/SBA-15	100 (100)	0 (0)	0 (0)	68 (65)	8 (6)	19 (29)	0.29	0.30	0.60

[a] The parenthesized values refer to the composition of particles on the surface of catalysts sulfided by the liquid-phase method [15].

Table 3. Catalytic properties of Mo(W)/SBA-15 catalysts in the 4,6-dimethyldibenzothiophene hydrodesulfurization

Catalyst	Conversion, %	Rate constant k_{HDS}, $\times 10^5$ mol g^{-1} h^{-1}	Selectivity $S_{HYD/DDS}$
Mo_{12}/SBA-15	26.7	11.6	6.4
W_{12}/SBA-15	11.7	4.5	5.9
Mo_3W_9/SBA-15	43.5	17.1	6.3
$(Mo_3 + W_9)$/SBA-15	35.7	13.5	5.4

compared with the liquid-phase sulfiding providing the use of dimethyl disulfide.

The bimetallic MoW/SBA-15 catalysts are distinguished by a higher activity in the 4,6-DMDBT hydrodesulfurization compared with the monometallic counterparts. The synergistic effects makes itself evident to a higher extent when mixed heteropoly acid are used as an oxide precursor. The turnover frequencies for the Mo_3W_9/SBA-15 catalyst are two times higher than the corresponding values for the reference samples. This indicates formation of a more active $MoWS_2$ sulfide phase. Thus, the use of the mixed heteropoly acid $H_4SiMo_3W_9O_{40}$ as an oxide precursor and mesostructured silica SBA-15 as a support allows one to synthesize the highly active hydrotreating catalyst.

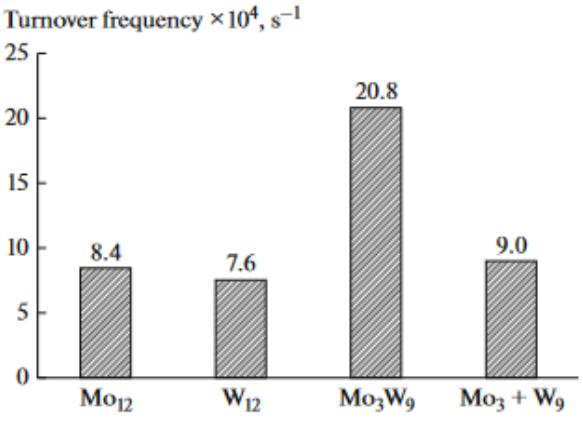

Fig. 2. Turnover frequency (TOF) in the 4,6-DMDBT hydrodesulfurization over edge active sites of Mo(W)S_2 crystallites in the Mo(W)/SBA-15 catalysts.

FUNDING

This work was supported by the Ministry of Education and Science of the Russian Federation (project no. 14.586.21.0054, unique project identifier RFMEFI58617X0054) and the Ministry of Foreign Affairs and International Development (France) and the Ministry of National Education, Higher Education, and Science (France) within the framework of the Partenariats Hubert Curien (PHC) program Kolmogorov for 2017–2019.

CONFLICT OF INTEREST

The authors declare that there is no conflict of interest.

ADDITIONAL INFORMATION

A.S. Koklukhin, ORCID: https://orcid.org/0000-0002-4737-120X

M.S. Nikul'shina, ORCID: https://orcid.org/0000-0001-7081-7049

A.A. Sheldaisov-Meshcheryakov, ORCID: https://orcid.org/0000-0001-7084-1583

A.V. Mozhaev, ORCID: https://orcid.org/0000-0003-3781-6073

C. Lancelot, ORCID: https://orcid.org/0000-0002-0691-0721

P. Blanchard, ORCID: https://orcid.org/0000-0003-0055-396X

C. Lamonier, ORCID: https://orcid.org/0000-0002-5100-8139

P.A. Nikul'shin, ORCID: https://orcid.org/0000-0002-3243-7835

REFERENCES

1. I. V. Babich and J. A. Moulijn, Fuel **82**, 607 (2003).
2. I. R. Yakupov, V. V. Yurchenko, A. V. Akhmetov, M. U. Imasheva, and A. F. Akhmetov, Nauchnye Trudy NIPI Neftegaz GNKAR, No. **2**, 68 (2015).
3. A. Stanislaus, A. Marafi, and M. Rana, Catal. Today **153**, 1 (2010).
4. B. Pawelec, R. M. Navarro, J. M. Campos-Martin, and J. L. G. Fierro, Catal. Sci. Technol. **1**, 23 (2011).
5. C. Thomazeau, C. Geantet, M. Lacroix, M. Danot, V. Harle, and P. Raybaud, Appl. Catal., A **322**, 92 (2007).
6. A. Tanimu and K. Alhooshani, Energy Fuels **34** (3), 2810 (2019).
7. P. Nikulshin, A. Mozhaev, C. Lancelot, P. Blanchard, E. Payen, and C. Lamonier, C. R. Chim., No. 19, 1276 (2016).
8. M. Breysse, C. Geantet, P. Afanasiev, J. Blanchard, and M. Vrinat, Catal. Today **130**, 3 (2008).
9. M. Nikulshina, A. Mozhaev, C. Lancelot, P. Blanchard, M. Marinova, C. Lamonier, and P. Nikulshin, Catal. Today **329**, 24 (2019).
10. J. Díaz de León, Kumar C. Ramesh, J. Antúnez-García, and S. Fuentes-Moyado, Catalysts **9**, 87 (2019).
11. L. Lizama and T. Klimova, Appl. Catal., B, No. 82, 139 (2008).
12. F. J. Méndez, A. Llanos, M. Echeverría, R. Jáuregui, Y. Villasana, Y. Díaz, G. Liendo-Polanco, M. A. Ramos-García, T. Zoltan, and J. L. Brito, Fuel, No. 110, 249 (2013).
13. B. Pawelec, S. Damyanova, R. Mariscal, J. L. G. Fierro, I. Sobrados, J. Sanz, and L. Petrov, J. Catal., No. 223, 86 (2004).
14. A. Kokliukhin, M. S. Nikulshina, A. Sheldaisov, Meshcheryakov, A. Mozhaev, and P. Nikulshin, J. Catal. Lett. **148**, 2869 (2018).
15. M. S. Nikulshina, A. V. Mozhaev, A. A. Sheldaisov-Meshcheryakov, and P. A. Nikulshin, Pet. Chem. **57** (12), 1058 (2017).
16. R. Shafi, M. Rafiq, H. Siddiqui, G. J. Hutchings, E. G. Derouane, and I. V. Kozhevnikov, Appl. Catal., A **204**, 251 (2000).
17. J. A. Mendoza-Nieto, F. Robles-Mendez, and T. Klimova, Catal. Today **250**, 47 (2015).
18. D. Zhao, Q. Huo, J. Feng, B. F. Chmelka, and G. D. Stucky, J. Am. Chem. Soc., No. 120, 6024 (1998).
19. P. Souchay, *Ions Mineraux Condenses* (Masson et Cie, Paris, 1969).
20. C. Rocchiccioli-Deltcheff, M. Fournier, R. Franck, and R. Thouvenot, Inorg. Chem., No. 22, 207 (1983).
21. S. Kasztelan, H. Toulhoat, J. Grimblot, and J. P. Bonnelle, Appl. Catal., No. 13, 127 (1984).
22. Y. Okamoto, K. Ochiai, M. Kawano, K. Kobayashi, and T. Kubota, Appl. Catal., A **226**, 115 (2002).
23. H. Toulhoat and P. Raybaud, Rev. Inst. Fr. Pet. 832 (2013).
24. P. A. Nikulshin, A. V. Mozhaev, K. I. Maslakov, A. A. Pimerzin, and V. M. Kogan, Appl. Catal., B 158–159, 161 (2014).
25. M. Nikulshina, A. Mozhaev, C. Lancelot, M. Marinova, P. Blanchard, E. Payen, C. Lamonier, and P. Nikulshin, Appl. Catal., B **224**, 951 (2018).
26. M. S. Nikulshina, P. Blanchard, A. Mozhaev, C. Lancelot, A. Griboval-Constant, M. Fournier, E. Payen, O. Mentre, V. Briois, P. A. Nikulshin, and C. Lamonier, Catal. Sci. Technol. **8**, 5557 (2018).

Translated by T. Soboleva